Drag Force on a Vertical Axis Wind Turbine with Airfoil Pitch Control

Junkun Ma
Department of Engineering Technology, Sam Houston State University, Huntsville, TX, USA

Introduction

This paper presents the study of the drag force acting on the central rotation axis of a Vertical Axis Wind Turbine (VAWT) consisting of three NACA0012 airfoils when subjecting to a transverse wind. Figure 1 shows a schematic representation of the turbine. VAWTs are easier to install and maintain since the central rotation axis is typically set transverse to the wind direction. Therefore, the generator and rotation transmission mechanisms can be placed at the base level, where it is close to the ground. An additional benefit of this setup is that there is no need to point it into the wind and thus reduce the associated systems and machine complexity [1]. Over the past few decades, various variations of this setup have been developed to overcome disadvantages such as low starting torque, low peak efficiency, narrow operating range, pulsatory torque, and dynamic instability [2,3]. Recently, researchers proposed pitch control systems such as the Self-Acting Stabilized Pitch Control, the Sinusoidal Forced Pitch Variation, and the Aero Pitch, etc. for VAWT system performance improvement. Experimental results have shown that they all can improve the starting torque, provide a broader operating range, and result in higher efficiency than the conventional VAWTs in which the airfoils are fixed to their supporting arm. However, in all the traditional and newer designs, the dynamic drag force acting on the rotation axis always exists.

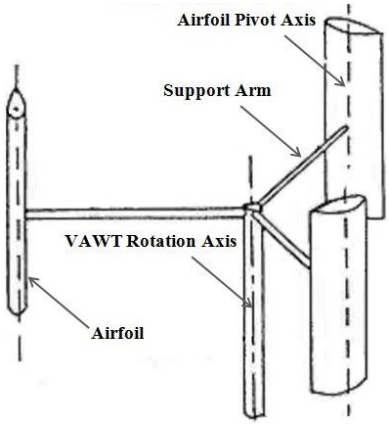

Figure 1 Schematic of a VAWT consisting of three NACA0012 airfoils with pitch control [4]

In this study, the CFD Module of the COMSOL Multiphysics® software is used to simulate the airflow around the three NACA0012 airfoils of a VAWT. Based on the total stress, pressure, and viscous stress on the airfoil surfaces obtained from the simulation, drag force acting on the VAWT rotation axis is calculated. Effects of pitch control on the drag force are also investigated as each of the airfoils is capable of pivoting individually with respect to their support arms that are fixed to the central rotation axis, and thus changing the angle of attack between the wind and the airfoils. The goal is to understand how the pitch control of the airfoils affects the drag force on the rotation axis of VAWTs.

A set of 2D models representing three NACA0012 airfoils (each has a chord length of one-meter) that are set at 120^0 apart along the circumference of a circular shape with one-meter radius is created and simulated using the COMSOL CFD™ module. The airfoils are pivoted with respect to the center of their chord lines to obtain wind attack angles ranging from 0^0 to 90^0 with a 10^0 increment, which represents the minimum to maximum torque contribution to the rotation of the central rotation axis [4]. The airfoils that are rotating up against the wind are always pivoted to a 0^0 wind attack angle and thus to minimize resistance to the rotation. The initial wind speed of 5m/s at the inlet and laminar flow are studied. The NACA0012 airfoils are modeled based on the shape function, as shown in Figure 2.

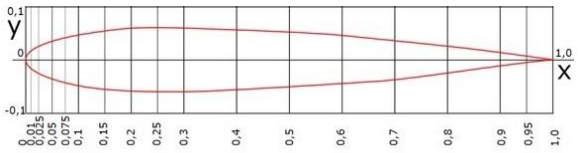

$$y = \pm 0.6\left[0.2969\sqrt{x} - 0.1260x - 0.3516x^2 + 0.2843x^3 - 0.1015x^4\right]$$

Figure 2 Shape function of a NACA0012 airfoil

Governing Equations

As a first approach, the flow around the airfoils is considered as laminar flow. The wind is treated as a homogeneous mass without impurities such as vapor or dust, and no shear is assumed. Since the low wind speed of 5m/s at the inlet is studied, the modeling is based on single-phase flow, which is governed by the general Navier-Stokes fluid flow that can be expressed by the following equations [5].

conservation of mass:

$$\frac{\partial \rho}{\partial t} + \nabla \cdot (\rho \boldsymbol{u}) = 0$$

conservation of momentum:

$$\rho\frac{\partial \boldsymbol{u}}{\partial t}+\rho(\boldsymbol{u}\cdot\nabla)\boldsymbol{u}=\nabla\cdot[-p\boldsymbol{I}+\tau]+\boldsymbol{F}$$

conservation of energy in the form of temperature:

$$\rho\boldsymbol{C}_p\left(\frac{\partial T}{\partial t}+(\boldsymbol{u}\cdot\nabla)T\right) = -(\nabla\cdot q)+\boldsymbol{\tau}:\boldsymbol{S} - \frac{T}{\rho}\frac{\partial\rho}{\partial T}\Big|_p\left(\frac{\partial p}{\partial t}+(\boldsymbol{u}\cdot\nabla)p\right)+Q$$

where (all in SI unit)

- ρ is the density (kg/m^3)
- $\boldsymbol{u}$ is the velocity vector (m/s)
- p is pressure (Pa)
- $\boldsymbol{\tau}$ is the viscous stress tensor (Pa)
- $\boldsymbol{F}$ is the volume force vector (N/m^3)
- Cp is the specific heat capacity at constant pressure ($J/(kg\cdot K)$)
- T is the absolute temperature (K)
- $\boldsymbol{q}$ is the heat flux vector (W/m^2)
- Q represents the heat source (W/m^3)
- $\boldsymbol{S}$ is the strain-rate tensor:

$$\boldsymbol{S}=\frac{1}{2}(\nabla\boldsymbol{u}+(\nabla\boldsymbol{u})^T)$$

and the operator ':' refers to double dot product representing a contraction between two tensors that is defined as:

$$\boldsymbol{a}:\boldsymbol{b}=\sum_n\sum_m a_{nm}b_{nm}$$

For a Newtonian fluid, the viscous stress can be expressed as:

$$\boldsymbol{\tau}=2\mu\boldsymbol{S}-\frac{2}{3}\mu(\nabla\cdot\boldsymbol{u})\boldsymbol{I}$$

where μ is the dynamic viscosity ($Pa\cdot s$). Airflow through the airfoils is also considered isothermal in this study.

Numerical Model

The COMSOL Multiphysics graphics user interface is used to model the geometry of the VAWT, and the CFD module is used to simulate the flow of air through the airfoils to find the velocity and pressure fields on the surface of these airfoils. The 2-D geometry consists of three NACA0012 airfoils that are set at 120^0 apart along the circumference of a circular shape with a one-meter radius represents the VAWT. The geometry of the support arms is not included and considered fixed at the central rotation axis located at the center of the circle. The support arms connect airfoils at their chord line centers, which are also the pivoting centers. The three airfoils are placed into a 12m by 6m rectangle area representing a wind tunnel. The top and bottom of the rectangle, as well as the surfaces of the three airfoils, are modeled as wall boundaries, while the left side of the rectangle is set as the inlet where a 5m/s transverse wind flows in, and the right side of the rectangle is set as an outlet.

To study the effects of pitch control on the airfoils, the support arm angle of the left-most airfoil is varied from 0^0 to 110^0 with a 10^0 increment (representing one-third of a complete rotation). Since the three airfoils are 120^0 apart, only one-third of a full rotation is required. At each support arm angle, the wind attack angle is pivoted from 0^0 to 90^0 with a 10^0 increment. The rotation is assumed to be counter-clockwise, and the airfoils positioned above the rotation axis are set to a 0^0 wind attack angle to minimize their resistance to the rotation while the ones located below the rotation axis are pivoted to the afore-mentioned different wind attack angles.

Figure 3 shows the definition of support arm angle and wind attack angle. Figure 4 shows the schematic representation of the COMSOL CFD model for the VAWT (the airfoils are set perpendicular to their supporting arms, and the left-most support arm is in the position with a 0^0 support arm angle). Figure 5 shows an example of the VAWT model with pitch control (40^0 support arm and 50^0 attack angles).

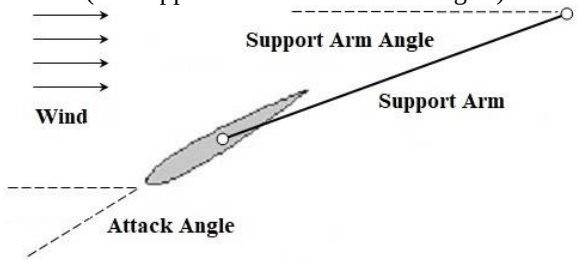

Figure 3 Definition of support arm & wind attack angles

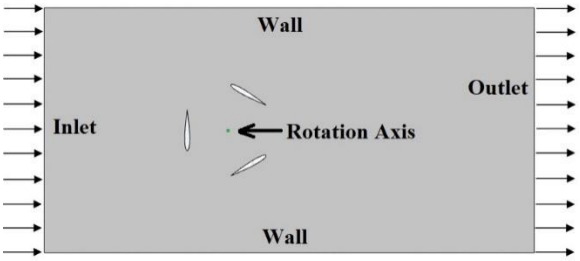

Figure 4 VAWT model with fixed airfoils

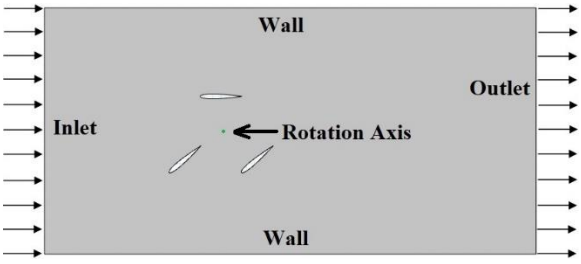

Figure 5 VAWT model with pitch control

Using the COMSOL CFD module, time-dependent studies are created to simulate the transit process from wind entering the inlet until the airflow around the airfoils reaches a steady status. Figure 6 shows a typical mesh optimized for the wall boundary conditions used for the simulation.

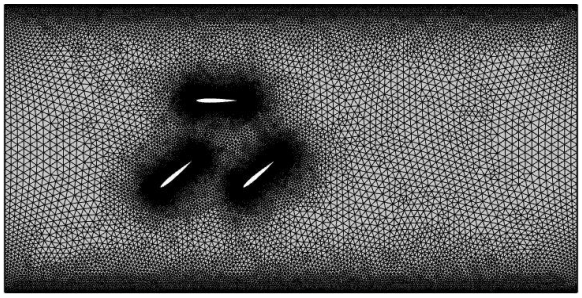

Figure 6 A representative mesh optimized for the wall boundary conditions

Generally, lift and drag forces are defined as the forces acting on objects that are perpendicular and parallel to the flow direction, respectively. These forces are created due to the pressure and viscous forces acting on the surface of the airfoils. The pressure force exists due to the airspeed difference and thus pressure gradient along the surface of the objects, while the viscous force is due to friction acting on the surface of the objects along the opposite direction of the flow. The lift and drag forces acting individual airfoil of the VAWT can be obtained by integrating the total stress components *spf.T_stressx* and *spf.T_stressy* along the airfoil surface and adjusted based on the wind attach angle *alpha* as *spf.T_stressx * sin(alpha*pi/180) – spf.T_stressy * cos(alpha*pi/180).* In this study, the drag force refers to the total force acting on the central rotation axis along the wind direction (horizontal) and the lift force is the force exerting on the same central rotation axis along the direction perpendicular to the wind flow (vertical). Therefore, in this study, there is no need to adjust the forces due to wind attack angle, which is required for individual airfoil. The pressure and viscous force components are also calculated separately by integrating the pressure components *p*spf.nxmesh* and *p*sp.nymesh* and viscous forces components *-spf.K_stressx* and *-spf.K_stressy* over the surfaces of the airfoils.

Results and Discussion

A set of time-dependent COMSOL CFD models representing various support arm and wind attack angles as described above are created to simulate the airflow through the VAWT airfoils. Based on the obtained total stress vector on the surface of the airfoils, drag and lift forces are obtained by integrating the total stress components along the surface of the airfoils. To exam the contribution of pressure and viscous flow to drag and lift forces, they are also calculated separately. The goal is to find out the effects of pitch control on the drag and lift forces acting on the central rotation axis. Selected representative results are presented below.

As an example, results for a 50^0 support arm angle (for the left-most airfoil) and 50^0 wind attack angle are shown below. Other combinations show similar trends. The velocity magnitude with streamline at 5 seconds since the start of the airflow is shown in Figure 8 (There are two airfoils positioned below the rotation axis, and thus both are pivoted to the 50^0 wind attack angle). Pressure field with velocity vectors is also shown in Figure 8. It can be seen that the three airfoils do affect the airflow around themselves, particularly the two pivoted ones.

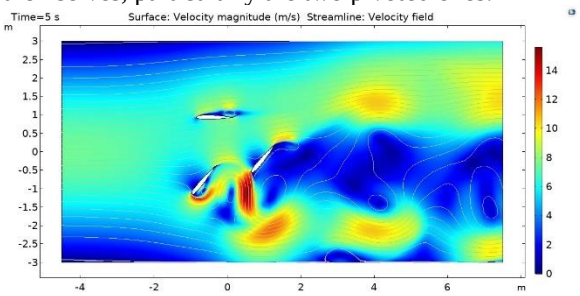

Figure 7 Velocity magnitude with streamline for 50^0 support arm and wind attack angles

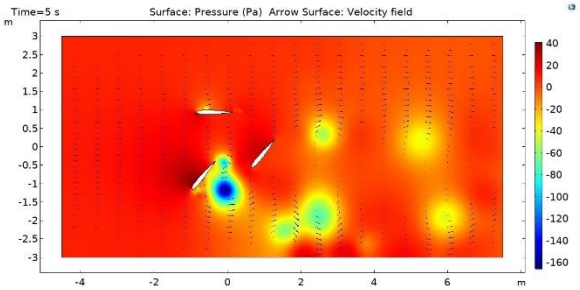

Figure 8 Pressure field and velocity vectors for 50^0 support arm and 50^0 wind attack angles

Integrating the total stress components *spf.T_stressx* and *spf.T_stressy* along the surface of the three airfoils, the drag force along the horizontal direction and the lift force along the vertical direction can be calculated, as shown in Figure 9. Figure 10 shows the drag and lift forces due to pressure and viscous force separately. It is evident that in both the drag and lift cases, the contributions of the viscous force are nearly zero. Both the drag and lift forces show an oscillating pattern and reach steady status after approximately four seconds. For this given support arm angle and wind attack angle combination, the drag force is always positive indicating that the drag is along the wind flow direction, while the lift force is negative suggesting a downward lift force along the

vertical direction. This is likely because the two pivoted airfoils both show a higher pressure on the upper half surfaces facing the wind than the other lower half surfaces in the back, as shown in Figure 8. The airfoil above the rotation axis is pivoted to a 0^0 wind attack angle to minimize its resistance to the rotation, and it shows minimal (but not zero) contribution to the drag but a significant amount to the lift as shown in Figure 11. This is due to the existence of the other airfoils causing disturbance of airflow and thus pressure difference between the top and bottom surfaces of this airfoil, and it is different from a single airfoil case in which the vertical force is also zero.

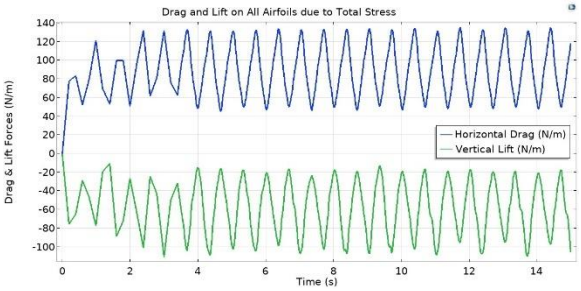

Figure 9 Drag and lift based on total stress

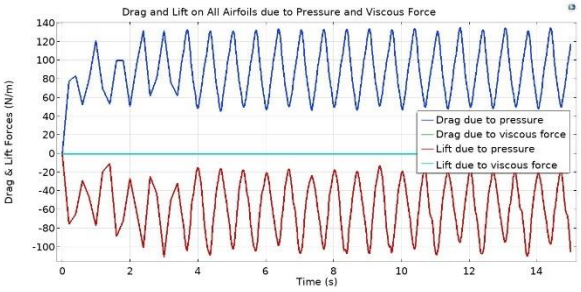

Figure 10 Drag and lift due to pressure and viscous force

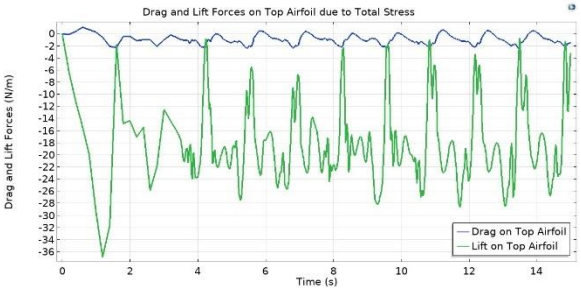

Figure 11 Drag and lift on the top airfoil due to total stress

To understand the effects of pitch control on the drag and lift forces as the VAWT rotates, CFD models to simulate airflow for the airfoils with a changing wind attack angle ranging from 0^0 to 90^0 and 0^0 to 110^0 support arm angle for the left-most airfoil are created, and time-dependent transit studies are conducted. When the support arm angle is changing between 0^0 and 60^0, two airfoils are positioned below the rotation axis and are pivoted to the same wind attack angle. When the support arm angle is changing between 70^0 and 110^0, only one airfoil is positioned below the rotation axis and pivoted to different wind attack angles. When the airfoils are positioned above the rotation axis, they are always oriented at 0^0 wind attack angle position. Figure 12 shows the pressure field and velocity vectors for 100^0 support arm angle and 50^0 wind attack angle.

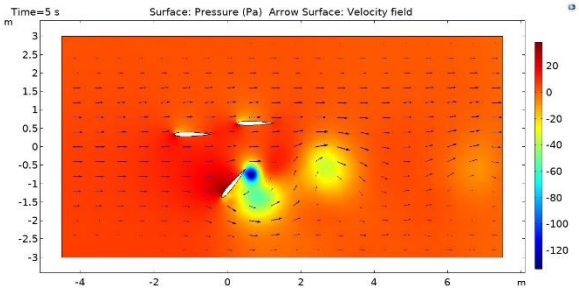

Figure 12 Pressure field and velocity vectors for 50^0 support arm and 50^0 wind attack angles

To compare the drag and lift forces due to different wind attack angles at a given support arm angle, the mean values and standard deviation of the drag and lift forces after four seconds since the start of flow (when the airflow is steady) are calculated. Figure 13 and Figure 14 shows representative examples of the effects of wind attack angle on drag and lift forces for support arm angles 0^0~60^0 (two airfoils pivoted) and 70^0 ~ 110^0 (only one airfoil pivoted) respectively. The data points on the graphs are the mean values, and the error bars indicate the range of variations.

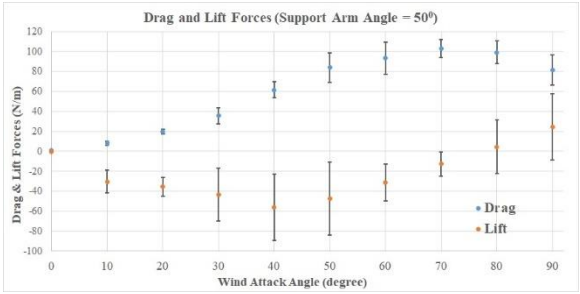

Figure 13 Effects of wind attack angle on drag and lift forces(support arm angle = 50^0)

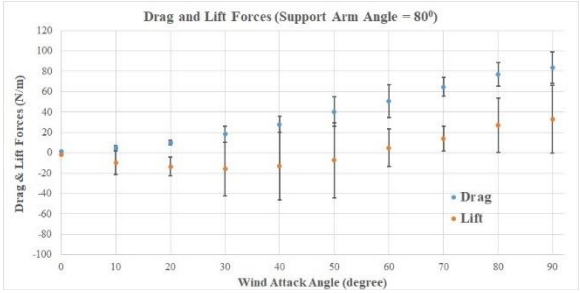

Figure 14 Effects of wind attack angle to drag and lift forces(support arm angle = 80^0)

The results show that the drag force for all the cases is always positive, indicating a horizontal force acting on the rotation axis along the wind flow direction, although the magnitudes vary. For the support arm angles that are 60^0 or less, the drag force increases initially and then decreases as the wind attack angle approaches 90^0. When the support arm angle is 70^0 or larger, the drag force continuously increases as the wind attack angle increases. The lift force shows negative values initially and then turns into positive as the wind attack angle increases for all combinations of wind attack angle and support arm angle.

Conclusions

From the results described above, with consideration of various combinations of support arm angle and wind attack angle, the following conclusions are drawn.

- Both drag and lift forces show an oscillating pattern as a function of time for all combinations of support arm angle and wind attack angle;
- Drag force is always positive indicating a horizontal force acting on the rotation axis along the wind flow direction with various magnitudes;
- Lift forces are initially negative and then change to positive, which means a downward and then upward vertical force acting on the rotation axis also with various magnitudes;
- When the support arm angle is 60^0 or less, two airfoils are below the rotation axis. They both are pivoted for pitch control and airflow around them interfere with each other. As a result, the drag force increases initially and then decreases depending on the combination of support arm angle and wind attack angle.

In this study, the physical geometry of support arms and rotation axis are not considered. Three-dimension model to include these elements, as well as consideration of edge effects of the airfoils, are necessary for further study.

References

1. A.R. Jha, Wind Turbine Technology, *CRC Press* (2010)
2. H.M. Drees, The cycloturbine and its potential for broad application, *2nd International Symposium on Wind Energy*, Amsterdam, Netherlands, Oct., (1978)
3. M.H. Khan, Model and prototype performance characteristics of Savonius rotor windmill, *Wind Engineering*, Vol. 2, No 2, p75-85, (1978)
4. J. Ma, C. Koutsougeras, and H. Luo, Efficiency of a Vertical Axis Wind Turbine (VAWT) with Airfoil Pitch Control, *COMSOL Conference 2017 Boston*, Oct. 4-6, (2017)
5. COMSOL Inc., Theory of Laminar Flow, COMSOL Multiphysics Reference Manual, COMSOL 5.4